

# Diffraction at HERA, Tevatron and LHC \*

CHRISTOPHE ROYON

IRFU-SPP, CEA Saclay, F91 191 Gif-sur-Yvette, France

In this short review, we describe some of the results on diffraction from the Tevatron and give some prospects for the LHC. In particular, we discuss the search for exclusive events at the Tevatron and their importance for the LHC program/ We finish by presenting the project of installing forward detectors in the ATLAS collaboration at 220 and 420 m.

PACS numbers: 12.38.Qk,13.85.Hd,14.70.Fm,14.80.Bn,14.80.Cp

## 1. Inclusive diffraction at HERA

In this short review, we will only describe briefly the measurement of the inclusive diffractive structure function  $F_2^D$  and the extraction of the gluon density of the Pomeron. A more detailed study can be found in Ref. [1].

In Fig. 1, we give an event display of a standard deep inelastic interaction (DIS) event (top) and from a diffractive one (bottom). For typical DIS events, the electron is scattered in the backward detector or the LAr calorimeter and the proton is destroyed. Part of the proton energy can be detected in the forward detectors such as the forward liquid argon calorimeter, the PLUG calorimeter or the forward muon detector. In about 10% of the events (see Fig. 1, bottom), the situation is different: there is no energy in the forward part of the detector. It means that there is no colour exchange between the proton and the jet produced in the event. In most of these events, the proton remains intact and is scattered at very small angle from the beam direction. This brings us to two different possibilities of detecting diffractive events, namely the rapidity gap selection where a gap devoid of energy is requested in the forward region of the detector, and the proton tagging detection where special detectors can be placed close to the beam in the very forward direction <sup>1</sup>.

---

\* Presented at the 2009 Epiphany Conference, Cracow, in honour of Jan Kwiecinski

<sup>1</sup> Another method developed by the ZEUS collaboration is based on the fact that non diffractive events are exponentially suppressed at high values of  $M_X$ , the total invariant mass produced in the event.

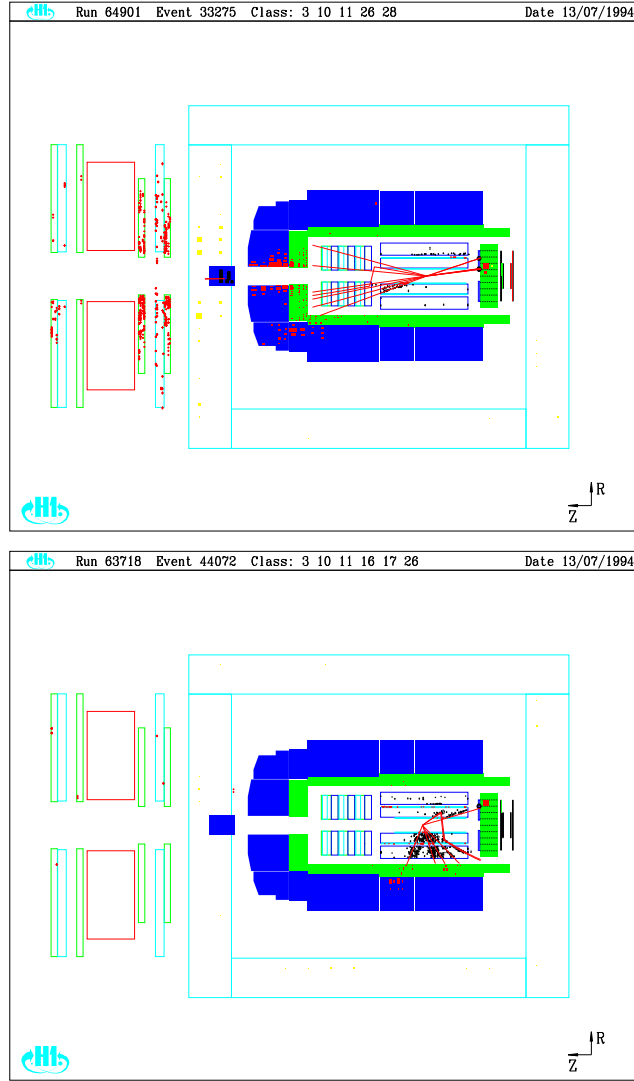


Fig.1. "Usual" and diffractive events in the H1 experiment.

The scheme of a diffractive event is shown in Fig. 2. In order to describe the diffractive processes where there is no colour exchange between the proton in the final state and the scattered jet, we have to introduce new variables in addition to the ones used to describe the inclusive DIS such as  $Q^2$ ,  $W$ ,  $x$  and  $y$ . Namely, we define  $x_P$ , which is the momentum fraction of the proton carried by the colourless object (called the pomeron), and  $\beta$ , the momentum fraction of the pomeron carried by the interacting parton inside the pomeron, if we assume the pomeron to be made of quarks and gluons

$$x_P = \xi = \frac{Q^2 + M_X^2}{Q^2 + W^2} \quad (1)$$

$$\beta = \frac{Q^2}{Q^2 + M_X^2} = \frac{x}{x_P}. \quad (2)$$

In the same way as the proton structure function is measured at HERA using DIS interactions, it is possible to measure the diffractive structure function for diffractive events [2]. Using the same analogy, it was proposed to perform a QCD DGLAP [3] (Dokshitzer Gribov Lipatov Altarelli Parisi) fit to the  $F_2^D$  data to extract the quark and gluon densities in the Pomeron if collinear and Regge factorisation are assumed [2, 4]. According to Regge theory, we can factorise the  $(x_P, t)$  dependence from the  $(\beta, Q^2)$  one for each trajectory (Pomeron and Reggeon). The diffractive structure function then reads:

$$F_2^D \sim f_p(x_P)(F_2^D)_{Pom}(\beta, Q^2) + f_r(x_P)(F_2^D)_{Reg}(\beta, Q^2) \quad (3)$$

where  $f_p$  and  $f_r$  are the pomeron and reggeon fluxes, and  $(F_2^D)_{Pom}$  and  $(F_2^D)_{Reg}$  the pomeron and reggeon structure functions. The flux parametrisation is predicted by Regge theory. The DGLAP QCD fit allows to obtain the parton distributions in the Pomeron as a direct output of the fit, and the gluon density is found to be much higher than the quark one, showing that the Pomeron is gluon dominated. The gluon density at high  $\beta$  is poorly constrained [2, 4].

## 2. Diffraction at Tevatron

At the Tevatron, diffraction can occur not only on either  $p$  or  $\bar{p}$  side as at HERA, but also on both sides. In the same way as the kinematical variables  $x_P$  and  $\beta$  are defined at HERA, we define  $\xi_{1,2}(=x_P \text{ at HERA})$  as the proton fractional momentum loss (or as the  $p$  or  $\bar{p}$  momentum fraction carried by the pomeron), and  $\beta_{1,2}$ , the fraction of the pomeron momentum carried by the interacting parton. The produced diffractive mass is equal to  $M^2 = s\xi_1$  for single diffractive events and to  $M^2 = s\xi_1\xi_2$  for double

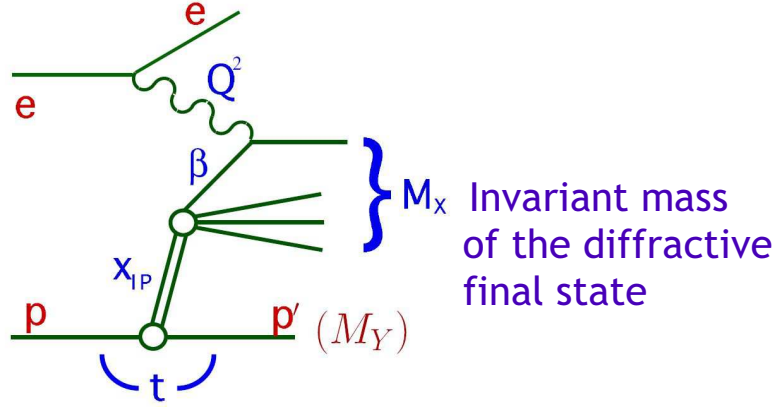


Fig. 2. Scheme of a diffractive event at HERA.

pomeron exchange where  $\sqrt{s}$  is the center-of-mass energy. The size of the rapidity gap is of the order of  $\Delta\eta \sim \log 1/\xi_{1,2}$ .

### 2.1. Factorisation breaking

A natural question to ask is whether one can use the diffractive PDFs extracted at HERA to describe hard diffractive processes in hadron-hadron collisions, and especially to predict the production of jets, heavy quarks or weak gauge bosons at the Tevatron.

From a theoretical point of view, diffractive hard-scattering factorization does not apply to hadron-hadron collisions because of additional interactions between the particles in initial and final states, as illustrated in Fig. 3. It is also worth noticing that the time scale when factorisation breaking occurs is completely different from the hard interaction one. Factorisation breaking is due to soft exchanges occurring in the initial and final states which appear at a much longer time scale than the hard interaction. In that sense, it is expected that the survival probability, defined as the probability that there is no soft additional interaction or in other words that the event remains diffractive, will not depend strongly on the type of hard interaction and its kinematics. In other words, the survival probability should be similar if one produces jets of different energies, vector mesons, photons, etc, which can be cross checked experimentally at Tevatron and LHC.

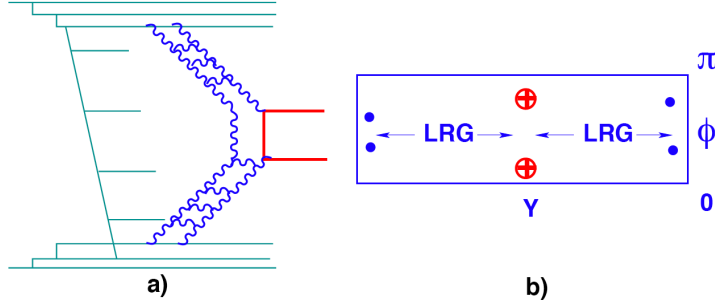


Fig. 3. Concept of survival probability.

## 2.2. Diffractive exclusive events and their interest at LHC

A schematic view of non diffractive, inclusive double pomeron exchange, exclusive diffractive events at the Tevatron or the LHC is displayed in Fig. 4. The upper left plot (1) shows the “standard” non diffractive events where the Higgs boson, the dijet or diphotons are produced directly by a coupling to the proton and shows proton remnants. The right plot (2) displays the standard diffractive double pomeron exchange where the protons remain intact after interaction and the total available energy is used to produce the heavy object (Higgs boson, dijets, diphotons...) and the pomeron remnants. There is a third class of processes displayed in the lower left figure (3), namely the exclusive diffractive production. In this kind of events, the full energy is used to produce the heavy object (Higgs boson, dijets, diphotons...) and no energy is lost in pomeron remnants.

There is an important consequence for the diffractive exclusive events: the mass of the produced object can be computed using forward detectors and tagged protons <sup>2</sup>

$$M = \sqrt{\xi_1 \xi_2 s} \quad (4)$$

where  $\sqrt{s}$  is the center-of-mass energy and  $\xi$  is the fraction of the proton momentum carried away by the Pomeron (called  $x_P$  at HERA). The advantage of those processes is obvious: we can benefit from the good forward detector resolution on  $\xi$  to get a good mass resolution, and to measure precisely the kinematical properties of the produced object.

<sup>2</sup> The formula is more complicated for low mass objects when the proton mass cannot be neglected [5].

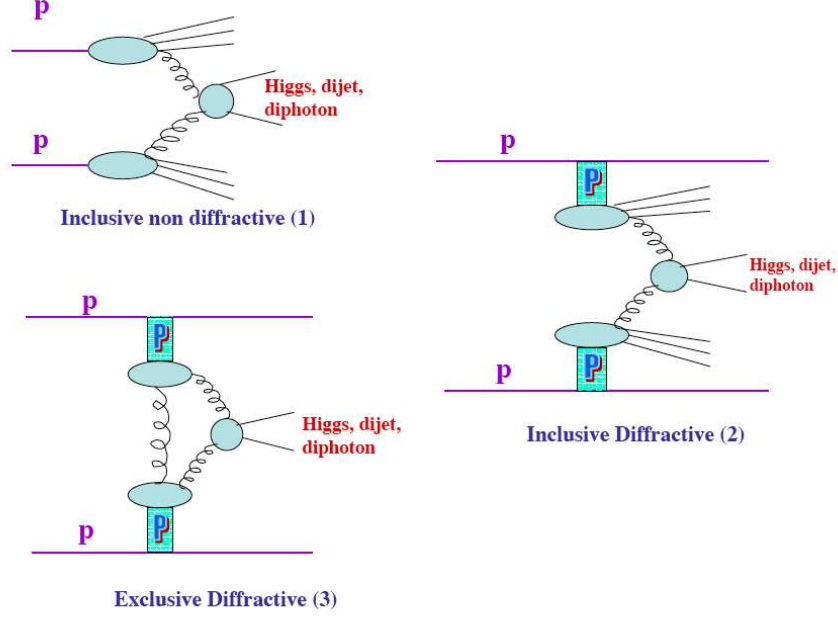


Fig. 4. Scheme of non diffractive, inclusive double pomeron exchange, exclusive diffractive events at the Tevatron or the LHC.

### 2.3. Search for diffractive exclusive events at the Tevatron

The CDF collaboration measured the so-called dijet mass fraction in dijet events — the ratio of the mass carried by the two jets produced in the event divided by the total diffractive mass — when the antiproton is tagged in the roman pot detectors and when there is a rapidity gap on the proton side to ensure that the event corresponds to a double pomeron exchange [6]. This measurement is compared to the expectation obtained from the pomeron structure in quarks and gluons as measured at HERA [4] (the factorisation breaking between HERA and the Tevatron is assumed to be constant and to come only through the gap survival probability, 0.1 at the Tevatron). The comparison between the CDF data for a jet  $p_T$  cut of 10 GeV as an example and the predictions from inclusive diffraction is given in Fig. 5, left, together with the effects of changing the gluon density at high  $\beta$  by changing the value of the  $\nu$  parameter. Namely, to study the uncertainty on the gluon density at high  $\beta$ , we multiply the gluon distribution by the factor  $(1 - \beta)^\nu$ . The  $\nu$  parameter varies between -1 and 1 (for  $\nu = -1$

(resp.  $+1$ ), the gluon density in the pomeron is enhanced (resp. damped) at high  $\beta$ ). QCD fits to the H1 data lead to an uncertainty on the  $\nu$  parameter of 0.5 [4]. Inclusive diffraction alone is not able to describe the CDF data at high dijet mass fraction, where exclusive events are expected to appear [7]. The conclusion remains unchanged when jets with  $p_T > 25$  GeV are considered.

Adding exclusive events to the distribution of the dijet mass fraction leads to a good description of data [7] as shown in Fig. 5, right. This does not prove that exclusive events exist but shows that some additional component with respect to inclusive diffraction compatible with exclusive events is needed to explain CDF data. To be sure of the existence of exclusive events, the observation will have to be done in different channels and the different cross sections to be compared with theoretical expectations.

Another interesting observable in the dijet channel is to look at the rate of  $b$  jets as a function of the dijet mass fraction. In exclusive events, the  $b$  jets are suppressed because of the  $J_Z = 0$  selection rule [8], and as expected, the fraction of  $b$  jets in the diffractive dijet sample diminishes as a function of the dijet mass fraction [6]).

The CDF collaboration also looked for the exclusive production of dilepton and diphoton [9]. Contrary to diphotons, dileptons cannot be produced exclusively via pomeron exchanges since  $gg \rightarrow \gamma\gamma$  is possible, but  $gg \rightarrow l^+l^-$  directly is impossible. Dileptons are produced via QED processes, and the CDF dilepton measurement is  $\sigma = 1.6_{-0.3}^{+0.5}(stat) \pm 0.3(syst)$  pb which is found to be in good agreement with QED predictions. 3 exclusive diphoton events have been observed by the CDF collaboration leading to a cross section of  $\sigma = 0.14_{-0.04}^{+0.14}(stat) \pm 0.03(syst)$  pb compatible with the expectations for exclusive diphoton production at the Tevatron. Unfortunately, the number of events is very small and the conclusion concerning the existence of exclusive events is uncertain. An update by the CDF collaboration with higher luminosity is however expected very soon. This channel will be however very important at the LHC where the expected exclusive cross section is much higher.

### 3. Exclusive diffraction at LHC

#### 3.1. Exclusive Higgs production at the LHC

One special interest of diffractive events at the LHC is related to the existence of exclusive events and the search for Higgs bosons at low mass in the diffractive mode. So far, two projects are being discussed at the LHC: the installation of forward detectors at 220 and 420 m in ATLAS and CMS [10] which we describe briefly at the end of this review.

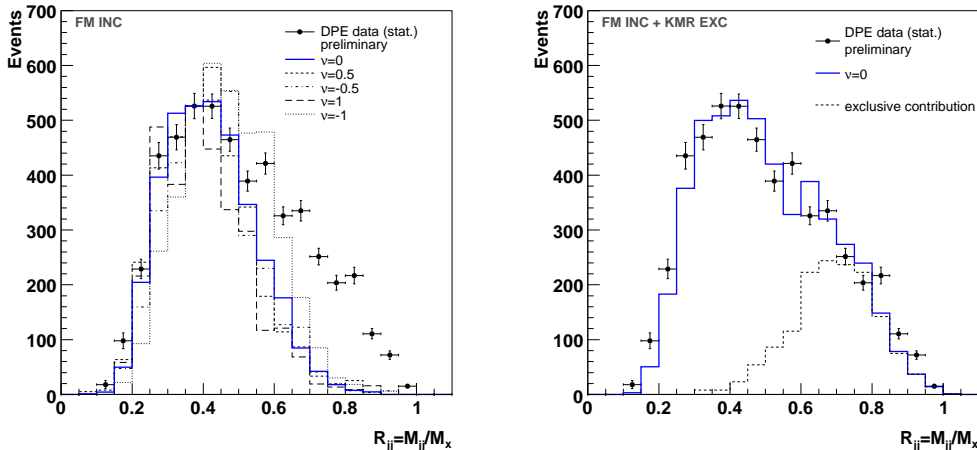


Fig. 5. Left: Dijet mass fraction measured by the CDF collaboration compared to the prediction from inclusive diffraction based on the parton densities in the pomeron measured at HERA. The gluon density in the pomeron at high  $\beta$  was modified by varying the parameter  $\nu$ . Right: Dijet mass fraction measured by the CDF collaboration compared to the prediction adding the contributions from inclusive and exclusive diffraction.

Many studies (including pile up effects and all background sources for the most recent ones) were performed recently [8, 11, 12] to study in detail the signal over background for MSSM Higgs production in particular. In Fig. 6, we give the number of background and MSSM Higgs signal events for a Higgs mass of 120 GeV for  $\tan \beta \sim 40$ . The signal significance is larger than  $3.5 \sigma$  for  $60 \text{ fb}^{-1}$  (see Fig. 6 left) and larger than  $5 \sigma$  after three years of data taking at high luminosity at the LHC and using timing detectors with a good timing resolution (see Fig. 6 right).

In some scenario such as NMSSM where the Higgs boson decays in  $h \rightarrow aa \rightarrow \tau\tau\tau\tau$  where  $a$  is the lighter of the two pseudo-scalar Higgs bosons, the discovery might come only from exclusive diffractive Higgs production [12] ( $m_a < 2m_b$  is natural in NMSSM with  $m_a > 2m_\tau$  somewhat preferred).

### 3.2. Photon induced processes at the LHC

In this section, we discuss particularly a new possible test of the Standard Model (SM) predictions using photon induced processes at the LHC, and especially  $WW$  production [13, 14]. The cross sections of these processes are computed with high precision using Quantum Electrodynamics (QED) calculations, and an experimental observation leading to differences with expectations would be a signal due to beyond standard model effects.



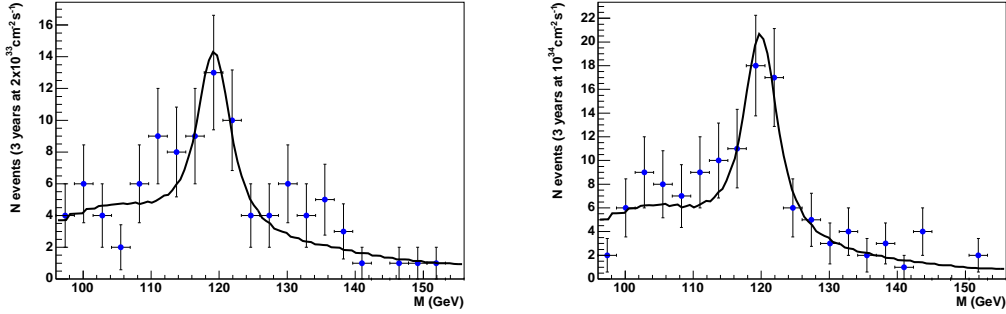


Fig. 6. Higgs signal and background obtained for MSSM Higgs production for neutral light CP-even Higgs bosons. The signal significance is larger than  $3.5 \sigma$  for  $60 \text{ fb}^{-1}$  (left plot) and larger than  $5 \sigma$  after three years of data taking at high luminosity at the LHC and using timing detectors with a resolution of 2 ps (right plot).

The experimental signature of such processes is the decay products of the  $W$  in the main central detectors from the ATLAS and CMS experiments and the presence of two intact scattered protons in the final state.

The main source of background is the  $W$  pair production in Double Pomeron Exchange (DPE). To remove most of the DPE background, it is possible to cut on the  $\xi$  of the protons measured in the proton taggers. Already with a low integrated luminosity of  $200 \text{ pb}^{-1}$  it is possible to observe 5.6  $W$  pair two-photon events for a background of DPE lower than 0.4, leading to a signal above  $8 \sigma$  for  $WW$  production via photon induced processes.

New physics with a characteristic scale (i.e. the typical mass of new particles) well above what can be probed experimentally at the LHC can manifest itself as a modification of gauge boson couplings due to the exchange of new heavy particles. The conventional way to investigate the sensitivity to the potential new physics is to introduce an effective Lagrangian with additional higher dimensional terms parametrized with anomalous parameters. We consider the modification of the  $WW\gamma$  triple gauge boson vertex with additional terms conserving  $C$ - and  $P$ - parity separately, that are parametrized with two anomalous parameters  $\Delta\kappa^\gamma, \lambda^\gamma$ . For  $30 \text{ fb}^{-1}$ , the reach on  $\Delta\kappa^\gamma$  and  $\lambda^\gamma$  is respectively 0.043 and 0.034, improving the direct limits from hadronic colliders by factors of 12 and 4 respectively (with respect to the LEP indirect limits, the improvement is only about a factor 2). Using a luminosity of  $200 \text{ fb}^{-1}$ , present sensitivities coming from the hadronic colliders can be improved by about a factor 30, while the LEP

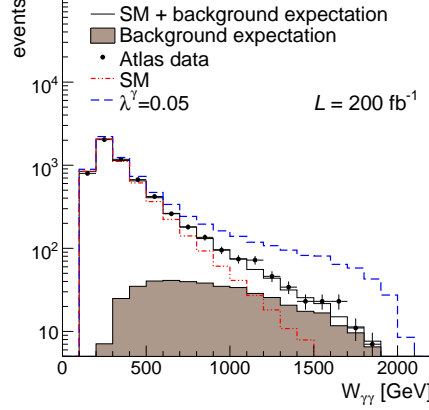


Fig. 7. Distributions of the  $\gamma\gamma$  photon invariant mass  $W_{\gamma\gamma}$  measured with the forward detectors using  $W_{\gamma\gamma} = \sqrt{s\xi_1\xi_2}$ . The effect of the  $\lambda^\gamma$  anomalous parameter appears at high  $\gamma\gamma$  invariant mass (dashed line). The SM background is indicated in dot-dashed line, the DPE background as a shaded area and their combination in full line. The black points show the ATLAS data smeared according to a Poisson distribution.

sensitivity can be improved by a factor 5.

It is worth noticing that many observed events are expected in the region  $W_{\gamma\gamma} > 1$  TeV where beyond standard model effects, such as SUSY, new strong dynamics at the TeV scale, anomalous coupling, etc., are expected (see Fig. 7). It is expected that the LHC experiments will collect 400 such events predicted by QED with  $W > 1$  TeV for a luminosity of  $200 \text{ fb}^{-1}$  which will allow to probe further the SM expectations. In the same way that we studied the  $WW\gamma$  coupling, it is also possible to study the  $ZZ\gamma$  one. The SM prediction for the  $ZZ\gamma$  coupling is 0, and any observation of this process is directly sensitive to anomalous coupling (the main SM production of exclusive  $ZZ$  event will be due to exclusive Higgs boson production decaying into two  $Z$  bosons if the Higgs boson exists in the relevant mass range). The  $WW$  cross section measurements are also sensitive to anomalous quartic couplings [15], and recent studies showed that the sensitivity on quartic coupling is 10000 times better than at LEP with only a luminosity of  $10 \text{ fb}^{-1}$ . In addition, it is possible to produce new physics beyond the Standard Model. Two photon production of SUSY leptons as an example has been investigated and the cross section for  $\gamma\gamma \rightarrow \tilde{l}^+\tilde{l}^-$  can be larger than 1 fb.

## 4. The AFP project at the LHC

### 4.1. Motivation

The motivation to install forward detectors in ATLAS and CMS is quite clear. Two locations for the forward detectors are considered at 220 and 420 m respectively to ensure a good coverage in  $\xi$  or in mass of the diffractively produced object as we will see in the following. Installing forward detectors at 420 m is quite challenging since the detectors will be located in the cold region of the LHC and the cryostat has to be modified to accomodate the detectors. In addition, the space available is quite small and some special mechanism called movable beam pipe are used to move the detectors close to the beam when the beam is stable enough. The situation at 220 m is easier since it is located in the warm region of the LHC. The AFP (ATLAS Forward Physics) project is under discussion in the ATLAS collaboration and includes both 220 and 420 m detectors on both sides of the main ATLAS detector.

The physics motivation of this project corresponds to different domains of diffraction which we already discussed:

- A better understanding of the inclusive diffraction mechanism at the LHC
- Looking for Higgs boson diffractive production in double pomeron exchange in the Standard Model or supersymmetric extensions of the Standard Model [8, 11] and measuring its properties (mass, spin...). This is clearly a challenging topic especially at low Higgs boson masses where the Higgs boson decays in  $b\bar{b}$  and the standard non-diffractive search is difficult.
- Sensitivity to the anomalous coupling of the photon by measuring the QED production cross section of  $W$  boson pairs [14].

### 4.2. Forward detector design and location

As we mentioned in the previous section, it is needed to install movable beam pipe detectors [10] at 220 and 420 m. The scheme of the movable beam pipe is given in Fig. 8. The principle developed originally for the ZEUS detector to tag electrons at low angle is quite simple and follows from the same ideas as the roman pots. The beam pipe is larger than the usual one and can host the sensitive detectors to tag the diffracted protons in the final state. When the beam is stable, the beam pipe can move so that the detectors can be closer to the beam. The movable beam pipe acts in a way as a single direction roman pot. In Fig. 8, we see the Beam Position Monitors (BPM) as well as the pockets where the detectors can be put. The

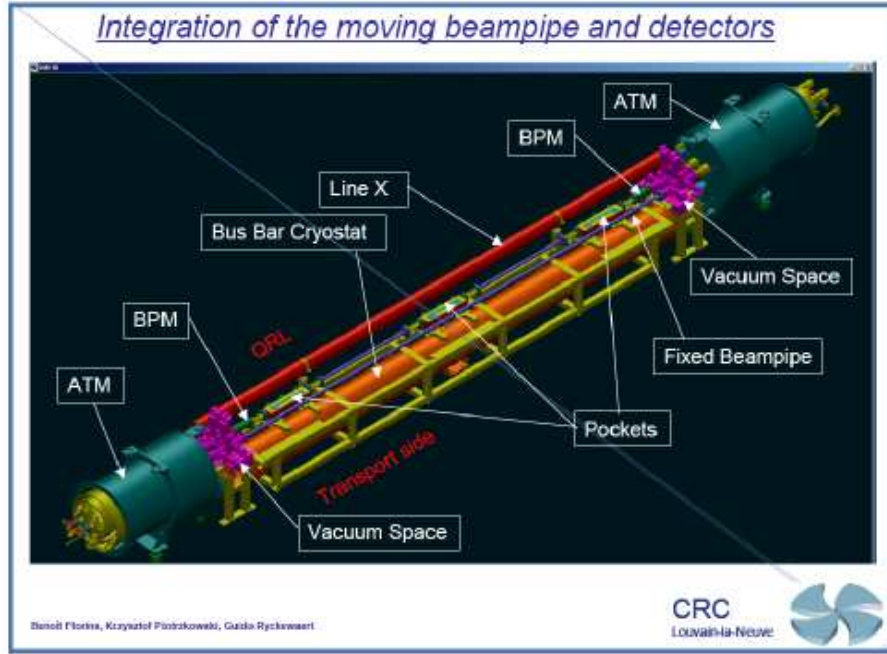


Fig. 8. Scheme of the movable beam pipe.

detectors can be aligned and calibrated using the BPMs as well as exclusive dimuon events. The dimuon mass can be well measured using the central muon detectors from ATLAS and can be compared to the result obtained using the missing mass method by tagging the final state proton in the forward detectors. This allows to calibrate the forward detectors by using data directly. The exclusive muon production cross section is expected to be high enough to allow this calibration on a store-by-store basis.

The missing mass acceptance is given in Fig. 9. The missing mass acceptance using only the 220 m pots starts at 135 GeV, but increases slowly as a function of missing mass. It is clear that one needs both detectors at 220 and 420 m to obtain a good acceptance on a wide range of masses since most events are asymmetric (one tag at 220 m and another one at 420 m). The precision on mass reconstruction using either two tags at 220 m or one tag at 220 m and another one at 420 m is of the order of 2-4 % on the full mass range, whereas it goes down to 1% for symmetric 420 m tags.

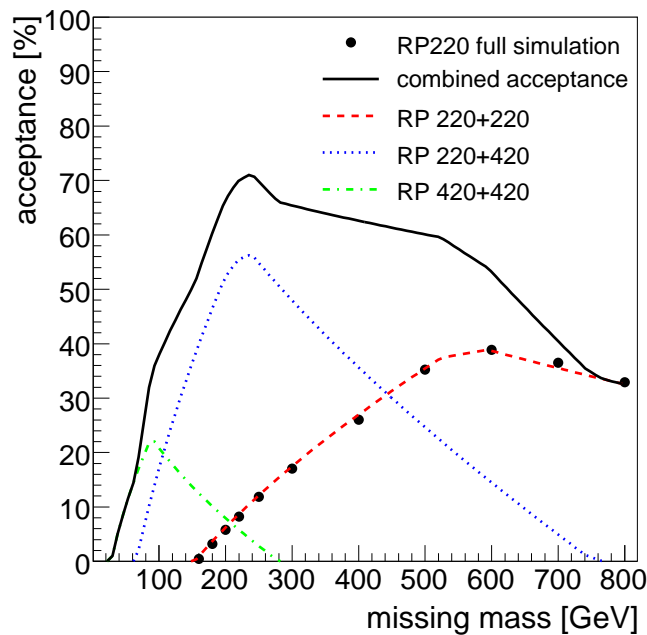


Fig. 9. Forward detector acceptance as a function of missing mass assuming a  $10\sigma$  operating positions, a dead edge for the detector of  $50\ \mu\text{m}$  and a thin window of  $200\ \mu\text{m}$ .

#### 4.3. Detectors inside forward detectors for the AFP project

We propose to put inside the forward detectors two kinds of detectors, namely 3D Silicon detectors to measure precisely the position of the diffracted protons, and the mass of the produced object and  $\xi$ , and precise timing detectors.

The position detectors will consist in 3D Silicon detector which allow to obtain a resolution in position better than  $10\ \mu\text{m}$ . The detector is made of 10 layers of 3D Si pixels of  $50 \times 400\ \mu\text{m}$ . One layer contains 9 pairs of columns of 160 pixels, the total size being  $7.2 \times 8\ \text{mm}^2$ . The detectors will be read out by the standard ATLAS pixel chip [10]. The latency time of the chip is larger than  $6\ \mu\text{s}$  which gives enough time to send back the local L1 decision from the forward detectors to ATLAS (see the next paragraph about trigger for more detail), and to receive the L1 decision from ATLAS, which means a distance of about 440 m. It is also foreseen to perform a slight modification of the chip to include the trigger possibilities into the chip.

The timing detectors are necessary at the highest luminosity of the LHC to identify from which vertex the protons are coming from. It is expected that up to 35 interactions occur at the same bunch crossing and we need to identify from which interaction, or from which vertex the protons are coming from. A precision of the order of 1 mm or 2-5 ps is required to distinguish between the different vertices and to make sure that the diffracted protons come from the hard interactions. Picosecond timing detectors are still a challenge and are developed for medical and particle physics applications. Two technologies are developed, either using as a radiator — with the aim to emit photons by the diffracted protons — or gas (gas Cerenkov detector or GASTOF) or a crystal of about 2.5 cm (QUARTIC), and the signal can be read out by Micro-Channel Plates Photomultipliers [10]. The space resolution of those detectors should be of the order of a few mm since at most two protons will be detected in those detectors for one given bunch crossing at the highest luminosity. The detectors can be read out with a Constant Fraction Discriminator which allows to improve the timing resolution significantly compared to usual electronics. A first version of the timing detectors is expected to be ready in 2010 with a resolution of 20-30 ps, and the final version by 2012-2013 with a resolution of 2-5 ps. The phototube aging due to the high proton rate at LHC at high luminosity is still an opened issue which is being solved in collaboration with the industry.

#### *4.4. Trigger principle and rate*

In this section, we would like to give the principle of the trigger using the forward detectors at 220 m as well as the rates obtained using a simulation of the ATLAS detector and trigger framework [10].

The principle of the trigger is shown in Fig. 10 in the case of a Higgs boson decaying into  $b\bar{b}$  as an example. The first level trigger comes directly from two different 3D Silicon layers in each forward detector. It is more practical to use two dedicated planes for triggering only since it allows to use different signal thresholds for trigger and readout. The idea is to send at most five strip addresses which are hit at level 1 (to simplify the trigger procedure, we group all pixels in vertical lines as one element only for the trigger since it is enough to know the distance in the horizontal direction to have a good approximation of  $\xi$ ). A local trigger is defined at the movable beam pipe level on each side of the ATLAS experiment by combining the two trigger planes in each movable beam pipe and the forward detectors as well. If the hits are found to be compatible (not issued by noise but by real protons), the strip addresses are sent to ATLAS, which allows to compute the  $\xi$  of each proton, and the diffractive mass. This information is then combined with the information coming from the central ATLAS

detector, requesting for instance two jets above 40 GeV in the case shown in Fig. 10. At L2, the information coming from the timing detectors for each diffracted proton can be used and combined with the position of the main vertex of ATLAS to check for compatibility. Once a positive ATLAS trigger decision is taken (even without any diffracted proton), the readout informations coming from the forward detectors are sent to ATLAS as any subdetector.

The different trigger possibilities for the forward detectors are given below:

- **Trigger on DPE events at 220 m:** This is the easiest situation since two protons can be requested at Level 1 at 220 m.
- **Trigger on DPE events at 220 and 420 m:** This is the most delicate scenario since the information from the 420 m pots cannot be included at L1 because of the L1 latency time of ATLAS. The strategy (see Table 1) is to trigger on heavy objects (Higgs...) decaying in  $b\bar{b}$  by requesting a positive tag (one side only) at 220 m with  $\xi < 0.05$  (due to the 420m RP acceptance in  $\xi$ , the proton momentum fractional loss in the 220m forward detector cannot be too high if the Higgs mass is smaller than 140 GeV), and topological cuts on jets such as the exclusiveness of the process  $((E_{jet1} + E_{jet2})/E_{calo} > 0.9$ ,  $(\eta_1 + \eta_2) \cdot \eta_{220} > 0$ , where  $\eta_{1,2}$  are the pseudorapidities of the two L1 jets, and  $\eta_{220}$  the pseudorapidity of the proton in the 220m movable beam pipe). This trigger can hold without prescales to a luminosity up to  $2.10^{33} \text{ cm}^{-2}\text{s}^{-1}$ , but would require an upgrade of the ATLAS L1 trigger. In addition, we are still looking at new possibilities to trigger in the same channels at higher luminosities. The ideas might be to use the layer 0 silicon or to the fact that  $b$  jets are thinner than gluon jets allowing a smaller sliding window. Let us note that the rate will be of the order of a few Hz at L2 by adding a cut on a presence of a tag in the 420 pots, on timing, and also on the compatibility of the rapidity of the central object computed using the jets or the protons in the forward detectors.

The trigger on  $W$ , top...will be given by ATLAS directly without any special forward trigger.

## 5. Conclusion

In this review, we described briefly the results on diffraction from Tevatron stressing in particular the search for diffractive exclusive events. This kind of events together with the QCD studies and the search for anomalous

$\mathcal{L}$ $E_T > 40 \text{ GeV}$	$n_{pp}$ per bunch crossing	2-jet rate [kHz] [ $\text{cm}^{-2} \cdot \text{s}^{-1}$ ]	RP200 reduction factor	$\xi < 0.05$ reduction factor	Jet Prop.
$1 \times 10^{32}$	0.35	2.6	120	300	1200
$1 \times 10^{33}$	3.5	26	8.9	22	88
$2 \times 10^{33}$	7	52	4.2	9.8	39.2
$5 \times 10^{33}$	17.5	130	1.9	3.9	15.6
$1 \times 10^{34}$	35	260	1.3	2.2	8.8

Table 1. L1 rates for 2-jet trigger with  $E_T > 40 \text{ GeV}$  and additional reduction factors due to the requirement of triggering on diffractive proton at 220 m, and also on jet properties. The total rate should not exceed a few kHz at L1.

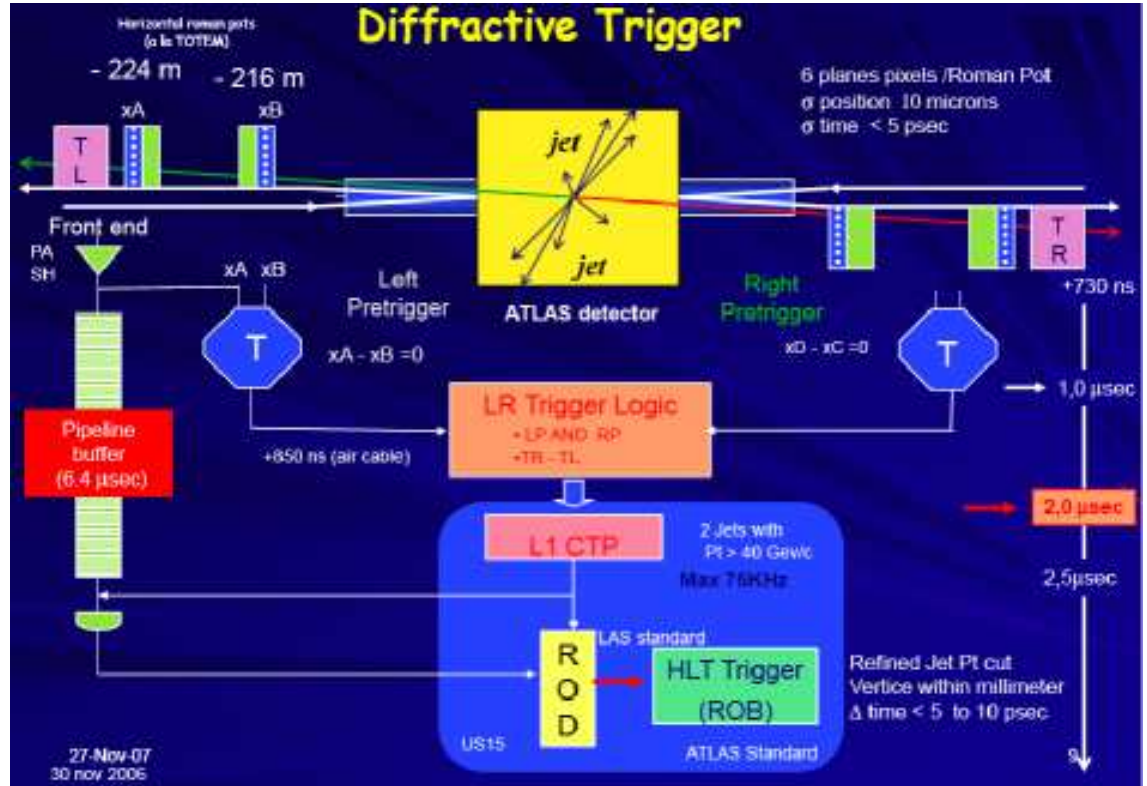


Fig. 10. Scheme for L1 trigger for the AFP project.

$\gamma W$  couplings motivated the project to install forward detectors in the ATLAS and CMS collaborations. These studies are only a small part of the



QCD studies which can be performed at the LHC concerning PDF [1] or low  $x$  resummation effects especially in the Mueller-Navelet or jet gap jet channels [16].

## REFERENCES

- [1] M. Boonekamp, F. Chevallier, C. Royon, L. Schoeffel, arXiv:0902.1678; C. Royon, *Acta Phys. Polon. B* **37** (2006) 3571; *Acta Phys. Polon. B* **39** (2008) 2339.; H. Abramowicz, contribution given at this conference.
- [2] H1 Collaboration, *Eur. Phys. J.* **C48** (2006) 715; *Eur. Phys. J.* **C48** (2006) 749; ZEUS Collaboration, *Nucl. Phys.* **B 713** (2005) 3.
- [3] G. Altarelli and G. Parisi, *Nucl. Phys.* **B126** 18C (1977) 298; V.N. Gribov and L.N. Lipatov, *Sov. Journ. Nucl. Phys.* (1972) 438 and 675; Yu.L. Dokshitzer, *Sov. Phys. JETP.* **46** (1977) 641.
- [4] C. Royon, L. Schoeffel, J. Bartels, H. Jung, R. Peschanski, *Phys. Rev.* **D63** (2001) 074004; C. Royon, L. Schoeffel, S. Sapeta, R. B. Peschanski and E. Sauvan, *Nucl. Phys. B* **781** (2007) 1 ; C. Royon, L. Schoeffel, R. B. Peschanski and E. Sauvan, *Nucl. Phys. B* **746** (2006) 15.
- [5] M. Rangel, C. Royon, G. Alves, J. Barreto, R. Peschanski, *Nucl. Phys.* **B774** (2007) 53.
- [6] CDF Collaboration, *Phys. Rev.* **D77** (2008) 052004.
- [7] O. Kepka, C. Royon, *Phys. Rev.* **D76** (2007) 034012.
- [8] C. Royon, *Mod. Phys. Lett. A* **18**, 2169 (2003) and references therein; M. Boonekamp, R. Peschanski, C. Royon, *Phys. Rev. Lett.* **87** (2001) 251806; *Nucl. Phys.* **B669** (2003) 277; M. Boonekamp, A. De Roeck, R. Peschanski, C. Royon, *Phys. Lett.* **B550** (2002) 93; V.A. Khoze, A.D. Martin, M.G. Ryskin, *Eur. Phys. J.* **C19** (2001) 477; *Eur. Phys. J.* **C23** (2002) 311; *Eur. Phys. J.* **C24** (2002) 581; arXiv:0802.0177; *Phys. Lett.* **B650** (2007) 41; A.B. Kaidalov, V.A. Khoze, A.D. Martin, M.G. Ryskin, *Eur. Phys. J.* **C33** (2004) 261; *Eur. Phys. J.* **C31** (2003) 387; R. Peschanski, M. Rangel, C. Royon, preprint arXiv:0808.1691.
- [9] CDF Collaboration, *Phys. Rev. Lett.* **99** (2007) 242002.
- [10] FP420 Coll., see <http://www.fp420.com>; ATLAS and CMS TDR to be submitted; see: <http://project-rp220.web.cern.ch/project-rp220/index.html>; C. Royon, preprint arXiv:0706.1796, proceedings of 15th International Workshop on Deep-Inelastic Scattering and Related Subjects (DIS2007), Munich, Germany, 16-20 Apr 2007.
- [11] M. Boonekamp, J. Cammin, S. Lavignac, R. Peschanski, C. Royon, *Phys. Rev.* **D73** (2006) 115011, and references therein.
- [12] B. Cox, F. Loebinger, A. Pilkington, *JHEP* **0710** (2007) 090; S. Heinemeyer et al., *Eur. Phys. J. C* **53** (2008) 231; J.R. Forshaw, J.F. Gunion, L. Hodgkinson, A. Papaefstathiou, A.D. Pilkington, *JHEP* **0804** (2008) 090.

- [13] M. Boonekamp, J. Cammin, R. Peschanski, C. Royon, Phys. Lett. **B654** (2007) 104.
- [14] O. Kepka, C. Royon, Phys. Rev. D **78** (2008) 073005.
- [15] E. Chapon, F. Chevallier, O. Kepka, C. Royon, in preparation; T. Pierzchala and K. Piotrkowski, arXiv:0807.1121 [hep-ph]; N. Schul and K. Piotrkowski, arXiv:0806.1097 [hep-ph].
- [16] H.Navelet, R.Peschanski, Ch.Royon, S.Wallon, Phys. Lett. **B385** (1996) 357; H. Navelet, R. Peschanski, C. Royon, Phys. Lett. B366 (1996) 329; A. Bialas, R. Peschanski, C. Royon, Phys. Rev. D **57** (1998) 6899; S. Munier, R. Peschanski, C. Royon, Nucl. Phys. B **534** (1998) 297; O. Kepka, C. Marquet, R. Peschanski and C. Royon, Phys. Lett. **B655** (2007) 236; Eur. Phys. J. **C55** (2008) 259; C. Marquet, C. Royon, Nucl. Phys. **B739** (2006) 131; Phys. Rev. **D79** (2009) 034028; G. Beuf, R. Peschanski, C. Royon, D. Salek, Phys. Rev. D78 (2008) 074004; F. Chevallier, O. Kepka, C. Marquet, C. Royon, arXiv:0903.4598.